

Formation of Benzene and Naphthalene through Cyclopentadienyl-Mediated Radical–Radical Reactions

Ralf I. Kaiser,* Long Zhao, Wenchao Lu, Musahid Ahmed,* Marsel V. Zagidullin, Valeriy N. Azyazov, and Alexander M. Mebel*



Cite This: *J. Phys. Chem. Lett.* 2022, 13, 208–213



Read Online

ACCESS |



Metrics & More

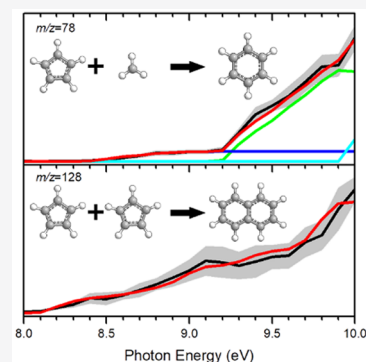


Article Recommendations



Supporting Information

ABSTRACT: Resonantly stabilized free radicals (RSFRs) have been contemplated as fundamental molecular building blocks and reactive intermediates in molecular mass growth processes leading to polycyclic aromatic hydrocarbons (PAHs) and carbonaceous nanoparticles on Earth and in deep space. By combining molecular beams and computational fluid dynamics simulations, we provide compelling evidence on the formation of benzene via the cyclopentadienyl-methyl reaction and of naphthalene through the cyclopentadienyl self-reaction, respectively. These systems offer benchmarks for the conversion of a five-membered ring to the 6π -aromatic (benzene) and the generation of the simplest 10π -PAH (naphthalene) at elevated temperatures. These results uncover molecular mass growth processes from the “bottom up” via RSFRs in high temperature circumstellar environments and combustion systems expanding our fundamental knowledge of the organic, hydrocarbon chemistry in our universe.



Since the discovery of the cyclopentadienyl radical ($C_5H_5^\bullet$) by Thrush (1956),^{1,2} resonantly stabilized free radicals (RSFRs)—organic radicals, such as propargyl ($C_3H_3^\bullet$), cyclopentadienyl ($C_5H_5^\bullet$), and benzyl ($C_7H_7^\bullet$), with the unpaired electron delocalized over multiple carbon atoms—have been proposed as key reactive intermediates in molecular mass growth processes to polycyclic aromatic hydrocarbons (PAHs) and carbonaceous nanostructures in combustion flames, along with circumstellar envelopes of carbon-rich asymptotic giant branch (AGB) stars and planetary nebulae as their descendants.^{3–11} PAHs are defined as organic molecules composed of multiple fused benzenoid rings. Whereas on Earth, PAHs and nanometer-sized soot particles are classified as carcinogenic byproducts liberated in incomplete combustion processes of fossil fuel,¹² in the interstellar medium, PAHs have been implicated in the abiotic syntheses of biorelevant molecules essential to the earliest forms of life.^{13–16} PAHs are also ubiquitous in carbonaceous chondrites, such as Allende, Murchison, and Orgueil and may account for up to 30% of the cosmic carbon budget.^{17,18} Classified as an electron-deficient transient radical with a single unpaired electron delocalized over five chemically equivalent methylidyne (CH) moieties,^{19,20} the cyclopentadienyl radical ($C_5H_5^\bullet$) has been suggested as a critical precursor to the simplest 6π and 10π aromatic molecules: benzene (C_6H_6 (1)) and naphthalene ($C_{10}H_8$ (2)) (Figure 1).

Although the formation pathways of benzene (1) and naphthalene (2) via methylation of cyclopentadienyl (reaction 1)^{5,21–24} and through the cyclopentadienyl radical self-reaction [reaction 2],^{25–27} respectively, have been explored computa-

tionally for decades (Supporting Information Introduction—Theoretical Calculations), experimental evidence on the outcome of the elementary gas phase reactions of free cyclopentadienyl radicals at high temperatures along with an isomer specific in situ identification of benzene (1) and naphthalene (2) is lacking (Table S1). Therefore, a high-level experimental study is imperative to untangle not only the initial bond-forming steps but also successive isomerization pathways of cyclopentadienyl radical reactions controlling the synthesis of benzene (1) and naphthalene (2) at elevated temperatures. This approach establishes an experimental benchmark for a fundamental understanding of the reactivity of RSFRs such as the prototype cyclopentadienyl and changes our perception how we contemplate pathways to aromatic structures through reactions of RSFRs in our universe.

Here, we provide evidence on the formation and isomer selective in situ identification of benzene (C_6H_6 (1)) and naphthalene ($C_{10}H_8$ (2)) through barrierless radical–radical reactions of the cyclopentadienyl radical ($C_5H_5^\bullet$) with methyl (CH_3^\bullet) [reaction 1] and cyclopentadienyl ($C_5H_5^\bullet$) [reaction 2], respectively. These systems represent benchmarks of RSFR reactions initiated by barrier-less carbon–carbon bond coupling leading to 5-methylcyclopenta-1,3-diene ($C_5H_5CH_3$,

Received: November 14, 2021

Accepted: December 27, 2021

Published: December 30, 2021



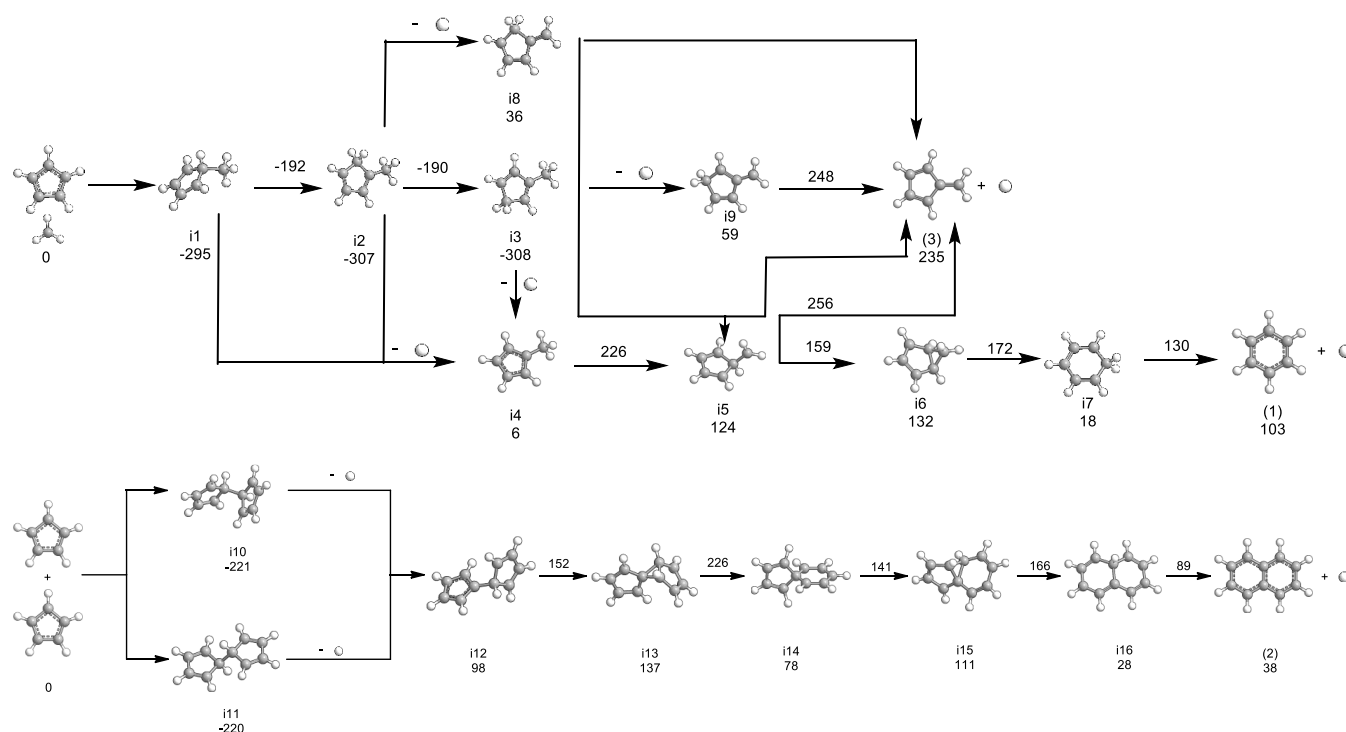
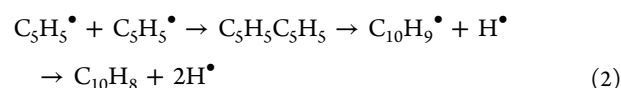
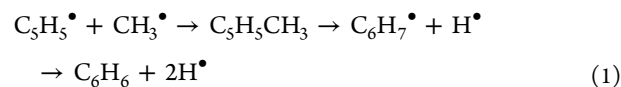


Figure 1. Top: Reaction pathways for the cyclopentadienyl–methyl system calculated at the CCSD(T)-F12/cc-pVTZ-f12 level theory extracted from ref 24. Bottom: Reaction pathways for the cyclopentadienyl radical self-reaction calculated at the G3(MP2,CC)//B3LYP/6-311G(d,p) level theory extracted from ref 26. The values on top of the arrows indicate transition state energies.

i11) and 9,10-dihydrofulvalene ($C_5H_5C_5H_5$, i10 and i11) intermediates, respectively (Figure 1). Atomic hydrogen loss succeeded by extensive isomerization through hydrogen migration, ring expansion, and ring contraction via exotic bicyclic reaction intermediates eventually form benzene (1) and naphthalene (2) under experimental conditions simulating the high temperature conditions of combustion systems and of carbon-rich circumstellar environments.²⁸ Supported by computational fluid dynamics (CFD) and kinetic simulations, the routes of methylation (reaction [1], Figure 1 top) and self-recombination (reaction [2], Figure 1 bottom) offer benchmarks for the conversion of a five-membered ring to a six-membered ring and for the synthesis of a bicyclic 10 π PAH. These routes bypass the “generally accepted” phenyl ($C_6H_5^\bullet$) radical mechanism via hydrogen abstraction–acetylene addition (HACA).^{29,30} Benzene (1) and naphthalene (2) along with the phenyl ($C_6H_5^\bullet$) and 1-/2-naphthyl ($C_{10}H_9^\bullet$) radicals, which are accessible via hydrogen abstraction as well as photolysis of 1 and 2, respectively, participate in molecular mass growth processes to truly complex PAHs and ultimately carbonaceous nanoparticles³¹ from the “bottom up”. This understanding of RSFR reactions is also crucial to decipher the low temperature chemistry that leads to carbon growth in hydrocarbon-rich atmospheres of planets and their moons. Although the initial step of each radical–radical recombination has no entrance barrier and proceeds rapidly, the low temperature prohibits the overall endoergic reactions. However, the low temperature and pressures of a few 100 Torr support three-body stabilizations of the collision complexes, which then can be photolyzed to eventually yield benzene (1) and naphthalene (2). These processes initiate fundamental mass growth processes, thus, providing the simplest aromatic building blocks for a rich photochemistry on a planetary scale.



Anisole ($C_6H_5OCH_3$) was used as a precursor to generate cyclopentadienyl ($C_5H_5^\bullet$) and methyl radicals (CH_3^\bullet) in well-defined molar ratios in the reactor;³² the products were identified with isomer selective synchrotron-based mass spectrometry through photoionization. Representative mass spectra, which provide information on the molecular formulas of the reaction products, were collected at a photoionization energy of 9.50 eV and temperature of 1525 ± 5 K (Figure 2). Control (blank) experiments of helium-seeded anisole ($C_6H_5OCH_3$) collected under identical experimental conditions, but without heating the silicon carbide tube, verify that the products are not contaminations from the reactants (Figure S1). The mass spectrum in Figure 2 reveals ion counts at $m/z = 64$ ($C_5H_4^+$), 65 ($C_5H_5^+$), 66 ($^{13}CC_4H_5^+/C_5H_6^+$), $m/z = 78$ ($C_6H_6^+$), 79 ($C_6H_7^+/^{13}CC_5H_6^+$), 80 ($C_6H_8^+$), 128 ($C_{10}H_8^+$), and 130 ($C_{10}H_{10}^+$). The aforementioned ions can be formally linked to $C_5H_5^\bullet$ (65 amu), a hydrogen loss product with the molecular formula C_5H_4 (64 amu), and the hydrogen atom addition product C_5H_6 (66 amu). Ion counts with lower intensities are magnified in the inset (Figure 2); these ion counts are absent in the control experiments highlighting that ions at $m/z = 78, 79, 80, 128,$ and 130 can be associated with the actual reaction products. Accounting for the molecular weights of these reactants, as well as the intermediates and products, C_6H_8 (80 amu) and $C_{10}H_{10}$ (130 amu) molecules are the result of the recombination of methyl (15 amu) with cyclopentadienyl (65 amu) (reaction 1) and of the cyclo-

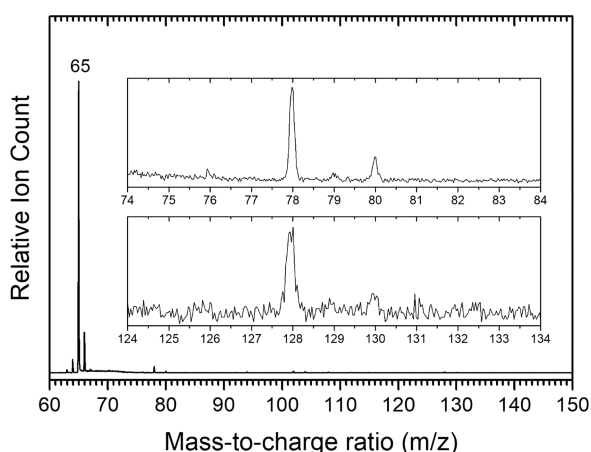


Figure 2. Photoionization mass spectrum recorded at a photon energy of 9.50 eV for the anisole/helium system at a temperature of 1525 ± 5 K. The inserts highlight the ion signal from $m/z = 74$ to 84 and $m/z = 124$ to 134.

pentadienyl self-recombination (reaction 2), respectively. Overall, two successive hydrogen atom losses could yield C_6H_6 (reaction 1) and $C_{10}H_8$ (reaction 2), the “target” products of this work.

It is the goal of the present work to identify not only the molecular formulas, but also the structural isomers formed in the cyclopentadienyl radical reactions 1 and 2. To accomplish this objective, we exploit photoionization efficiency curves (PIE), which report the intensity of a well-defined ion of a specific m/z ratio as a function of photon energy from 8.0 to 10.0 eV in steps of 0.05 eV (Figures 3 and S2). Each PIE graph can be fit with a (linear combination of) reference curves of distinct structural isomers, which serve as base functions. First, the PIE curve at $m/z = 78$, can be replicated by the sum of three C_6H_6 isomers: benzene (1), fulvene (3), and 1,5-hexadiyne (4) (Figure 3, Supporting Information). The onset of the ion counts at 8.40 ± 0.05 eV correlates nicely with the adiabatic ionization energy (IE) of fulvene (3) of 8.36 ± 0.02 eV.³³ The contribution of fulvene to the ion counts up to 9.2 eV is critical. From 9.2 to 9.9 eV, the incorporation of benzene is necessary to replicate the experimental data. The second onset of 9.2 eV agrees well with the adiabatic IE of benzene (1) of 9.25 ± 0.05 eV.³⁴ A contribution of 1,5-hexadiyne (4) with an adiabatic IE of 9.95 ± 0.05 eV is required to replicate

the section from 9.9 to 10.0 eV of the PIE curve of $m/z = 78$. Second, the PIE curve at $m/z = 79$ essentially overlaps with the PIE curve of $m/z = 78$ after scaling indicating that $m/z = 79$ represents the ^{13}C analogues of $m/z = 78$. Finally, the PIE curve at $m/z = 128$ can be reproduced with a single contribution from naphthalene (2). The onset of the ion counts at 8.1 eV agrees well with the adiabatic IE of naphthalene of 8.144 ± 0.001 eV.³⁵ Azulene, the structural isomer of naphthalene, is not formed; this isomer has an adiabatic IE of 7.42 ± 0.05 eV, but no ion counts are observed below 8.1 eV. The ion counts at $m/z = 128$ are weaker by a factor of about five compared to $m/z = 78$. Hence, due to the limited signal-to-noise, no reliable PIE curve for $m/z = 129$ ($^{13}CC_9H_5^+$) could be extracted.

This present examination provides direct evidence on the first gas phase preparation and in situ detection of the simplest monocyclic and bicyclic aromatics—benzene (1) and naphthalene (2)—through the reactions of the cyclopentadienyl with the methyl radical (reaction 1) and via the cyclopentadienyl radical self-reaction (reaction 2). The findings hold critical consequences to the chemistry of a key class of organic radicals, namely, RSFRs, and of aromatic systems in general in high temperature combustion flames and carbon-rich circumstellar envelopes of AGB stars. These complex chemical systems are driven by a series of bimolecular and termolecular reactions yielding eventually PAHs and carbonaceous nanoparticles (soot, interstellar grains). Barrierless bimolecular reactions 1 and 2 lead to 5-methylcyclopentadiene (1,3-diene (C_6H_8 , i1) and *cis/trans*-9,10-dihydrofulvalene (*cis/trans* $C_{10}H_{10}$, i10/i11) via recombination of the reactants with their radical centers resulting in the formation of a carbon–carbon single bond (Figure 1). In the cyclopentadienyl-methyl system, to form benzene (1), adduct i1 has to eventually emit a hydrogen atom yielding i4 or has to isomerize to i2 and i3 prior to ejecting a hydrogen atom to i8 and i9, respectively (Figure 1). For the cyclopentadienyl self-reaction, in order to access naphthalene (2), an atomic hydrogen elimination leading to i12 represents a critical prerequisite, too. These pathways to the hydrogen loss doublet radicals (i4, i8, i9, i12) are overall endoergic by 6 to 98 kJ mol^{-1} ; the endoergicities can be compensated by the high temperatures of combustion and circumstellar environments of a few 1000 K. Further, in combustion flames, the high-density conditions support three-body collisions and can also lead to a stabilization of the reaction intermediates (i1–i3, i10–i11). Krasnoukhov et al.

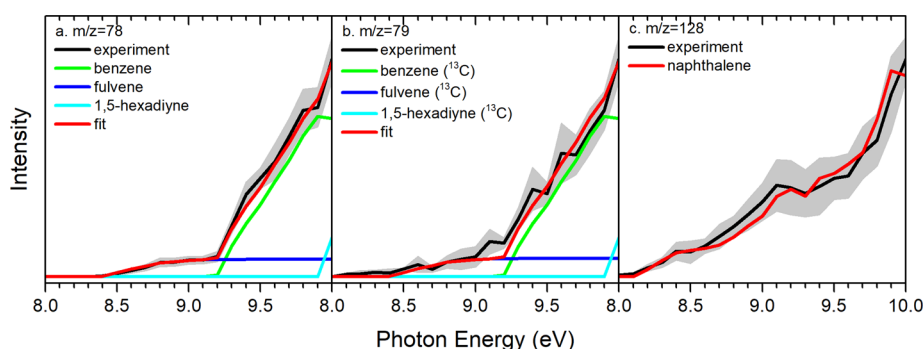


Figure 3. Photoionization efficiency (PIE) curves for products of interest in the reaction of the cyclopentadienyl radical with methyl (a and b) and the cyclopentadienyl radical self-recombination (c) at a reactor temperature of 1525 ± 5 K. Black: experimental PIE curves; blue/green/red: reference PIE curves; the red line resembles the overall fit. The error bars consist of two parts: $\pm 10\%$ based on the accuracy of the photodiode and a 1σ error of the PIE curve averaged over the individual scans.

revealed that at 760 Torr, nearly all collision complexes can be stabilized via third-body collisions.²³ The doublet radicals (**i4**, **i8**, **i9**, **i12**) are also accessible through hydrogen abstraction by, for example, atomic hydrogen, which represents a ubiquitous reactant in combustion systems. Further rearrangements of the radicals eventually lead to benzene (**1**) along with fulvene (**3**) (reaction 1 and naphthalene (**2**) (reaction 2). It is important to highlight that the branching ratio of benzene (**1**) versus fulvene (**3**) strongly depends on the pressure and the temperature. For example, at 1100 K and 7.6 Torr, branching ratios of 73% (**1**) and 27% (**2**) were predicted to be formed; as the pressure rises, the branching ratio of **1** versus **2** decreases. Similarly, when the temperature increases to 2000 K at 7.6 Torr, the predicted branching ratio of **1** drops to 61%, with that of **2** rising to 39%. At 1 atm, the **1** versus **2** branching ratio decreases from 70% to 30% at 1100 K to 42% to 58% at 2000 K.²⁴ We do acknowledge that Yuan et al. identified benzene and naphthalene during the pyrolysis of 1% anisole in 99% argon buffer gas at temperatures up to 1160 K in a flow reactor.³⁶ However, the present study was conducted under dilute reactant conditions of about 0.02% anisole providing methyl and cyclopentadienyl reactants at identical concentrations in helium. This low concentration along with a residence time of the reactants in our reactor of only a few tens of microseconds compared to hundreds of milliseconds in Yuan et al.'s flow reactor support an identification of initial products and eliminates molecular mass growth processes beyond naphthalene in the present study. Supported by fluid dynamics simulations, these dilute conditions are critical to extract information on the nascent, initial reaction pathways to benzene and naphthalene.³⁸

The trends of our high temperature experimental studies are fully supported by computational fluid dynamics (CFD) and kinetic simulations of the micro reactor (Supporting Information). These simulations model the temperature and pressure profiles (Figure S3) within the reactor and also incorporate a kinetic reaction model to rationalize the experimentally derived branching ratios of the reaction products (Figure 4, Tables S2 and S3). The legitimacy of this approach has been validated earlier by benchmarking the formation of naphthalene ($C_{10}H_8$) and [4]-helicene ($C_{18}H_{12}$).^{28,37} These simulations incorporate the key reaction

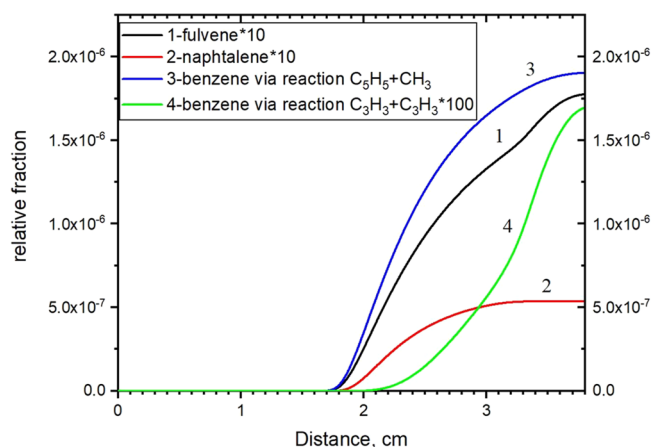


Figure 4. Growth of fulvene, naphthalene, and benzene along the distance within the pyrolytic reactor: (1) fulvene, (2) naphthalene, and (3) benzene via reaction 1; 4-benzene via propargyl radical self-reaction, involving reactions 6–21 (Table S2).

pathways predicted computationally by Krasnoukhov et al. (Figure 1 top)³⁸ and the detailed cyclopentadienyl radical self-reaction by Green and co-workers (Figure 1 bottom)²⁵ by focusing on reactions, which can actually produce benzene and their isomers, or naphthalene. More specifically, the reaction of cyclopentadienyl (C_5H_5) with methyl forming C_6H_8 intermediates was in fact implicitly included as the source of the rate constants;²⁴ this framework treated all pertinent reactions on the C_6H_8 and C_6H_7 surfaces including rate constants for the formation of benzene and fulvene. Further, the cyclopentadienyl (C_5H_5) self-reaction leading to $C_{10}H_{10}$ intermediates, which react via $C_{10}H_9$ to naphthalene ($C_{10}H_8$) was incorporated.²⁵ The $C_5H_5 + C_2H_2$, $CH_3 + CH_3$, $C_6H_5O + C_6H_5O$ reactions produce neither benzene nor naphthalene and were not included. Our simulations yield five key findings. First, these simulations replicate the higher yield of benzene (**1**) versus fulvene (**3**). Second, they reveal a strong preference of benzene (**1**) over naphthalene (**2**) (Figure 4). Third, the simulations reveal that 99% of benzene (**1**) is formed via reaction 1, whereas only 1% is formed via the propargyl radical self-reaction.³⁹ This can be rationalized considering that the formation of benzene (**1**) via the propargyl radical self-reaction is a “higher order” reaction since it requires the decomposition of the cyclopentadienyl radical to propargyl plus acetylene. This small fraction is also in line with the low ion counts of 1,5-hexadiyne ($HCCCH_2CH_2CCH$, **4**) formed via the recombination of two propargyl radicals at their CH_2 moieties.³⁹ Overall, we can conclude that the propargyl radical self-reaction only contributes to a minor amount of the overall benzene signal. Fourth, the $C_6H_7 + C_2H_2$ reaction is irrelevant since C_6H_7 is unstable under the micro reactor conditions rapidly equilibrating with C_6H_6 isomers plus atomic hydrogen. Fifth, the HACA growth from benzene to naphthalene was also eliminated by the modeling, since the addition of the HACA reactions in the model did not affect the yield of naphthalene.

The low temperature chemistry in the hydrocarbon-rich atmospheres of planets and their moons, such as Titan (80–150 K), represents a particular challenge for radical–radical reactions. Although the initial radical–radical recombination to 5-methylcyclopenta-1,3-diene (C_6H_8 , **i1**) and *cis/trans*-9,10-dihydrofulvalene (*cis/trans*- $C_{10}H_{10}$, **i10/i11**) have no entrance barrier and hence proceeds rapidly, the low temperature prohibits the overall endoergic unimolecular decomposition via atomic hydrogen loss or hydrogen abstraction generating the doublet radicals (**i4**, **i8**, **i9**, **i12**). However, the low temperature and pressures of a few 100 Torr support three-body stabilizations of the collision complexes by, for example, the nitrogen molecules in Titan’s atmosphere.⁴⁰ The stabilized collision complexes can then be photolyzed by photons of sufficient energy to eventually yield not only the required doublet radicals (**i4**, **i8**, **i9**, **i12**), but also eventually benzene (**1**), along with fulvene (**3**) and naphthalene (**2**). Commencing with **i1** and **i10/i11**, the transition states of highest energy reside at 543 and 318 kJ mol^{-1} , respectively, which requires photons of at least 5.63 (220 nm) and 3.30 eV (376 nm), respectively; these are readily available from the solar photon field interacting with Titan’s atmosphere. Once formed, benzene (**1**) and naphthalene (**2**) can be photolyzed to the phenyl ($C_6H_5^\bullet$) and 1-/2-naphthyl radicals ($C_{10}H_9^\bullet$). These radicals drive fundamental mass growth processes to anthracene ($C_{14}H_{10}$) and phenanthrene ($C_{14}H_{10}$)⁴¹ and beyond³¹ via low-temperature ring annulation upon reaction

with vinylacetylene (C_4H_4) thus providing the feedstock for a rich photochemistry on a planetary scale.

To conclude, the in situ identification of benzene (C_6H_6 (1)) and naphthalene ($C_{10}H_8$ (2)) showcases the critical importance of radical–radical reactions involving resonantly stabilized cyclopentadienyl radicals in the formation of the simplest 6π and 10π aromatic hydrocarbons under high temperature conditions mimicking combustion systems and circumstellar envelopes of carbon rich AGB stars like IRC +10216 along with planetary nebulae, such as CRL618 as their descendants.^{42–45} These processes facilitate molecular mass growth processes via methyl-radical induced ring expansion through the conversion of a five-membered ring to a six-membered ring molecule benzene (C_6H_6 (1)) and essentially bypass the high temperature HACA mechanism through cyclopentadienyl radical self-reaction to naphthalene ($C_{10}H_8$ (2)) thus providing unusual but experimentally substantiated pathways to PAH formation in high temperature environments. The reaction of the methyl radical with any cyclopentadienyl radical moiety incorporated into larger PAH structures is expected to eventually yield via ring expansion a six-membered ring; likewise, the reaction of the cyclopentadienyl radical with any cyclopentadienyl moiety of an aromatic substructure eventually transforms into a naphthalene structure incorporated within an existing aromatic molecule. Both processes essentially drive the formation of graphitic nanostructures and may provide a rationale of the synthesis and detection of graphite in carbonaceous meteorites,^{41,46,47} such as the L3 chondrite Khohar⁴⁸ and Murchison.⁴⁹ Therefore, the fundamental mechanistic pathways presented here will be crucial in rationalizing elementary reactions in complex chemical systems at high temperatures such as combustion and circumstellar environments one reaction at a time eventually enriching our knowledge of the formation and evolution of carbonaceous matter in the galaxy.

■ ASSOCIATED CONTENT

SI Supporting Information

The Supporting Information is available free of charge at <https://pubs.acs.org/doi/10.1021/acs.jpcllett.1c03733>.

Experimental methods, theoretical calculations and experiments, fluid dynamics calculation results, tables (previous studies, list of reactions, and rate constants), and figures (mass spectra, PIE curves, and CFD simulation) (PDF)

■ AUTHOR INFORMATION

Corresponding Authors

Ralf I. Kaiser – Department of Chemistry, University of Hawaii at Manoa, Honolulu, Hawaii 96822, United States; orcid.org/0000-0002-7233-7206; Email: ralfk@hawaii.edu

Musahid Ahmed – Chemical Sciences Division, Lawrence Berkeley National Laboratory, Berkeley, California 94720, United States; orcid.org/0000-0003-1216-673X; Email: mahmed@lbl.gov

Alexander M. Mebel – Department of Chemistry and Biochemistry, Florida International University, Miami, Florida 33199, United States; orcid.org/0000-0002-7233-3133; Email: mebela@fiu.edu

Authors

Long Zhao – Department of Chemistry, University of Hawaii at Manoa, Honolulu, Hawaii 96822, United States

Wenchao Lu – Chemical Sciences Division, Lawrence Berkeley National Laboratory, Berkeley, California 94720, United States; orcid.org/0000-0002-3798-5128

Marsel V. Zagidullin – Lebedev Physical Institute, Samara Branch, Samara 443011, Russian Federation

Valeriy N. Azyazov – Lebedev Physical Institute, Samara Branch, Samara 443011, Russian Federation

Complete contact information is available at: <https://pubs.acs.org/10.1021/acs.jpcllett.1c03733>

Notes

The authors declare no competing financial interest.

■ ACKNOWLEDGMENTS

This work was supported by the U.S. Department of Energy, Basic Energy Sciences DE-FG02-03ER15411 (experimental studies; L.Z., R.I.K.) and DE-FG02-04ER15570 (computational studies; A.M.M.) to the University of Hawaii and Florida International University, respectively. W.L. and M.A. are supported by the Director, Office of Science, Office of Basic Energy Sciences, of the U.S. Department of Energy under Contract No. DE-AC02-05CH11231, through the Gas Phase Chemical Physics program of the Chemical Sciences Division. The ALS is supported under the same contract. The CFD and kinetic simulations at the Lebedev Physical Institute were supported by the Ministry of Higher Education and Science of the Russian Federation under Grant No. 075-15-2021-597 (MVZ, VNA).

■ REFERENCES

- (1) Thrush, B. A. Spectrum of the cyclopentadienyl radical. *Nature* **1956**, *178* (4525), 155–156.
- (2) Engleman Jr, R.; Ramsay, D. A. Electronic absorption spectrum of the cyclopentadienyl radical (C_5H_5) and its deuterated derivatives. *Can. J. Phys.* **1970**, *48* (8), 964–969.
- (3) Miller, J. A. Theory and modeling in combustion chemistry. *Proc. Combust. Inst.* **1996**, *26* (1), 461–480.
- (4) Barker, J. R.; Frenklach, M.; Golden, D. M. When rate constants are not enough. *J. Phys. Chem. A* **2015**, *119* (28), 7451–7461.
- (5) Knyazev, V. D.; Popov, K. V. Kinetics of the self reaction of cyclopentadienyl radicals. *J. Phys. Chem. A* **2015**, *119* (28), 7418–7429.
- (6) Lemmens, A. K.; Rap, D. B.; Thunnissen, J. M. M.; Willemsen, B.; Rijs, A. M. Polycyclic aromatic hydrocarbon formation chemistry in a plasma jet revealed by IR-UV action spectroscopy. *Nat. Commun.* **2020**, *11* (1), 269.
- (7) Kukkadapu, G.; Wagnon, S. W.; Pitz, W. J.; Hansen, N. Identification of the molecular-weight growth reaction network in counterflow flames of the C_3H_4 isomers allene and propyne. *Proc. Combust. Inst.* **2021**, *38* (1), 1477–1485.
- (8) Peeters, E.; Mackie, C.; Candian, A.; Tielens, A. G. G. M. A spectroscopic view on cosmic PAH emission. *Acc. Chem. Res.* **2021**, *54* (8), 1921–1933.
- (9) Johansson, K. O.; Head-Gordon, M. P.; Schrader, P. E.; Wilson, K. R.; Michelsen, H. A. Resonance-stabilized hydrocarbon-radical chain reactions may explain soot inception and growth. *Science* **2018**, *361* (6406), 997–1000.
- (10) Baroncelli, M.; Mao, Q.; Galle, S.; Hansen, N.; Pitsch, H. Role of ring-enlargement reactions in the formation of aromatic hydrocarbons. *Phys. Chem. Chem. Phys.* **2020**, *22* (8), 4699–4714.

- (11) Miller, J. A.; Pilling, M. J.; Troe, J. Unravelling combustion mechanisms through a quantitative understanding of elementary reactions. *Proc. Combust. Inst.* **2005**, *30* (1), 43–88.
- (12) Chang, Y.; Rager, J. E.; Tilton, S. C. Linking coregulated gene modules with polycyclic aromatic hydrocarbon-related cancer risk in the 3D human bronchial epithelium. *Chem. Res. Toxicol.* **2021**, *34* (6), 1445–1455.
- (13) Keheyan, Y.; Aquilanti, V.; Brucato, J. R.; Colangeli, L.; Cataldo, F.; Mennella, V. Astrochemical and prebiological elementary processes. In *Exo-/astro-biology*, Proceedings of the First European Workshop, 21–23 May 2001, ESRIN, Frascati, Italy; Ehrenfreund, P., Angerer, O., Battrick, B., Eds.; ESA Publications Division: Noordwijk, 2001; Vol. SP-496, pp 357–361.
- (14) Ziurys, L. M. The chemistry in circumstellar envelopes of evolved stars: Following the origin of the elements to the origin of life. *Proc. Natl. Acad. Sci. U.S.A.* **2006**, *103* (33), 12274–12279.
- (15) Allamandola, L. J. PAHs and astrobiology. *EAS Publications Series* **2011**, *46*, 305–317.
- (16) d'Ischia, M.; Manini, P.; Moracci, M.; Saladino, R.; Ball, V.; Thissen, H.; Evans, R. A.; Puzzarini, C.; Barone, V. Astrochemistry and astrobiology: Materials science in wonderland? *Int. J. Mol. Sci.* **2019**, *20* (17), 4079–0.
- (17) Ehrenfreund, P.; Sephton, M. A. Carbon molecules in space: From astrochemistry to astrobiology. *Faraday Discuss.* **2006**, *133* (0), 277–288.
- (18) Tielens, A. G. G. M. Interstellar polycyclic aromatic hydrocarbon molecules. *Annu. Rev. Astron. Astrophys.* **2008**, *46*, 289–337.
- (19) Wentrup, C.; Crow, W. D. Structures of cyanocyclopentadienes and related compounds. *Tetrahedron* **1970**, *26* (18), 4375–4386.
- (20) Yi, W.; Chattopadhyay, A.; Bersohn, R. Unimolecular dissociation of cyclopentadiene and indene. *J. Chem. Phys.* **1991**, *94* (9), 5994–5998.
- (21) Moskaleva, L.; Mebel, A.; Lin, M. The $\text{CH}_3 + \text{C}_5\text{H}_5$ reaction: A potential source of benene at high temperatures. *Proc. Combust. Inst.* **1996**, *26* (1), 521–526.
- (22) Melius, C. F.; Colvin, M. E.; Marinov, N. M.; Pit, W. J.; Senkan, S. M. Reaction mechanisms in aromatic hydrocarbon formation involving the C_5H_5 cyclopentadienyl moiety. *Proc. Combust. Inst.* **1996**, *26* (1), 685–692.
- (23) Sharma, S.; Green, W. H. Computed rate coefficients and product yields for $\text{c-C}_5\text{H}_5 + \text{CH}_3$ products. *J. Phys. Chem. A* **2009**, *113* (31), 8871–8882.
- (24) Krasnoukhov, V. S.; Porfiriev, D. P.; Zavershinskiy, I. P.; Azyazov, V. N.; Mebel, A. M. Kinetics of the $\text{CH}_3 + \text{C}_5\text{H}_5$ reaction: A theoretical study. *J. Phys. Chem. A* **2017**, *121* (48), 9191–9200.
- (25) Long, A. E.; Merchant, S. S.; Vandeputte, A. G.; Carstensen, H.-H.; Vervust, A. J.; Marin, G. B.; Van Geem, K. M.; Green, W. H. Pressure dependent kinetic analysis of pathways to naphthalene from cyclopentadienyl recombination. *Combust. Flame* **2018**, *187*, 247–256.
- (26) Kislov, V. V.; Mebel, A. M. The formation of naphthalene, azulene, and fulvalene from cyclic C5 species in combustion: An ab initio/RRKM study of 9-H-fulvalenyl ($\text{C}_5\text{H}_5-\text{C}_5\text{H}_4$) radical rearrangements. *J. Phys. Chem. A* **2007**, *111* (38), 9532–9543.
- (27) Cavallotti, C.; Polino, D. On the kinetics of the $\text{C}_5\text{H}_5 + \text{C}_3\text{H}_5$ reaction. *Proc. Combust. Inst.* **2013**, *34* (1), 557–564.
- (28) Zagidullin, M. V.; Kaiser, R. I.; Porfiriev, D. P.; Zavershinskiy, I. P.; Ahmed, M.; Azyazov, V. N.; Mebel, A. M. Functional relationships between kinetic, flow, and geometrical parameters in a high-temperature chemical microreactor. *J. Phys. Chem. A* **2018**, *122* (45), 8819–8827.
- (29) Frenklach, M.; Feigelson, E. D. Formation of polycyclic aromatic hydrocarbons in circumstellar envelopes. *Astrophys. J.* **1989**, *341*, 372–384.
- (30) Parker, D. S.; Kaiser, R. I.; Troy, T. P.; Ahmed, M. Hydrogen Abstraction/Acetylene Addition Revealed. *Angew. Chem., Int. Ed.* **2014**, *53* (30), 7740–7744; *Angew. Chem.* **2014**, *126*, 7874–7878.
- (31) Kaiser, R. I.; Hansen, N. An aromatic universe—a physical chemistry perspective. *J. Phys. Chem. A* **2021**, *125* (18), 3826–3840.
- (32) Shaper, M.; Ramphal, I. A.; Neumark, D. M. Photodissociation of the cyclopentadienyl radical at 248 nm. *J. Phys. Chem. A* **2018**, *122* (17), 4265–4272.
- (33) Bieri, G.; Burger, F.; Heilbronner, E.; Maier, J. P. Valence Ionization Energies of Hydrocarbons. *Helv. Chim. Acta* **1977**, *60* (7), 2213–2233.
- (34) Duncan, M. A.; Dietz, T. G.; Smalley, R. E. Two-color photoionization of naphthalene and benzene at threshold. *J. Chem. Phys.* **1981**, *75* (5), 2118–2125.
- (35) Cockett, M. C. R.; Ozeki, H.; Okuyama, K.; Kimura, K. Vibronic coupling in the ground cationic state of naphthalene: A laser threshold photoelectron [zero kinetic energy (ZEKE) photoelectron] spectroscopic study. *J. Chem. Phys.* **1993**, *98* (10), 7763–7772.
- (36) Yuan, W.; Li, T.; Li, Y.; Zeng, M.; Zhang, Y.; Zou, J.; Cao, C.; Li, W.; Yang, J.; Qi, F. Experimental and kinetic modeling investigation on anisole pyrolysis: Implications on phenoxy and cyclopentadienyl chemistry. *Combust. Flame* **2019**, *201*, 187–199.
- (37) Zhao, L.; Kaiser, R. I.; Xu, B.; Ablikim, U.; Ahmed, M.; Zagidullin, M. V.; Azyazov, V. N.; Howlader, A. H.; Wnuk, S. F.; Mebel, A. M. VUV photoionization study of the formation of the simplest polycyclic aromatic hydrocarbon: Naphthalene (C_{10}H_8). *J. Phys. Chem. Lett.* **2018**, *9* (10), 2620–2626.
- (38) Mebel, A. M.; Landera, A.; Kaiser, R. I. Formation Mechanisms of Naphthalene and Indene: From the Interstellar Medium to Combustion Flames. *J. Phys. Chem. A* **2017**, *121*, 901–926.
- (39) Zhao, L.; Lu, W.; Ahmed, M.; Zagidullin, M. V.; Azyazov, V. N.; Morozov, A. N.; Mebel, A. M.; Kaiser, R. I. Gas-phase synthesis of benzene via the propargyl radical self-reaction. *Sci. Adv.* **2021**, *7* (21), No. eabf0360.
- (40) Trainer, M. G.; Jimenez, J. L.; Yung, Y. L.; Toon, O. B.; Tolbert, M. A. Nitrogen incorporation in CH_4 - N_2 photochemical aerosol produced by far ultraviolet irradiation. *Astrobiology* **2012**, *12* (4), 315–326.
- (41) Zhao, L.; Kaiser, R. I.; Xu, B.; Ablikim, U.; Ahmed, M.; Evseev, M. M.; Bashkurov, E. K.; Azyazov, V. N.; Mebel, A. M. Low-temperature formation of polycyclic aromatic hydrocarbons in Titan's atmosphere. *Nat. Astron.* **2018**, *2* (12), 973.
- (42) Cernicharo, J.; Heras, A. M.; Tielens, A.; Pardo, J. R.; Herpin, F.; Guelin, M.; Waters, L. Infrared Space Observatory's discovery of C_4H_2 , C_6H_2 , and benzene in CRL 618. *Astrophys. J.* **2001**, *546* (2), L123–L126.
- (43) Woods, P. M.; Millar, T. J.; Zijlstra, A. A.; Herbst, E. The synthesis of benzene in the proto-planetary nebula CRL 618. *Astrophys. J.* **2002**, *574* (2), L167–L170.
- (44) Woods, P. M.; Millar, T. J.; Zijlstra, A. A.; Herbst, E. The chemistry of CRL 618. In *Planetary Nebulae: Their Evolution and Role in the Universe*, Kwok, S., Dopita, M., Sutherland, R., Eds.; 2003; pp 279–280.
- (45) Boechat-Roberty, H. M.; Neves, R.; Pilling, S.; Lago, A. F.; de Souza, G. G. B. Dissociation of the benzene molecule by ultraviolet and soft X-rays in circumstellar environment. *Mon. Not. R. Astron. Soc.* **2009**, *394* (2), 810–817.
- (46) Yang, T.; Kaiser, R. I.; Troy, T. P.; Xu, B.; Kostko, O.; Ahmed, M.; Mebel, A. M.; Zagidullin, M. V.; Azyazov, V. N. HACA's heritage: A free-radical pathway to phenanthrene in circumstellar envelopes of Asymptotic Giant Branch Stars. *Angew. Chem.* **2017**, *56* (16), 4515–4519.
- (47) Kalpana, M.; Babu, E.; Mani, D.; Tripathi, R.; Bhandari, N. Polycyclic aromatic hydrocarbons in the Mukundpura (CM2) Chondrite. *Planet. Space Sci.* **2021**, *198*, 105177.
- (48) Mostefaoui, S.; Hoppe, P.; El Goresy, A. In situ discovery of graphite with interstellar isotopic signatures in a chondrule-free clast in an L3 chondrite. *Science* **1998**, *280* (5368), 1418–1420.
- (49) Zinner, E.; Amari, S.; Wopenka, B.; Lewis, R. S. Interstellar graphite in meteorites: Isotopic compositions and structural properties of single graphite grains from murchison. *Meteoritics* **1995**, *30* (2), 209–226.